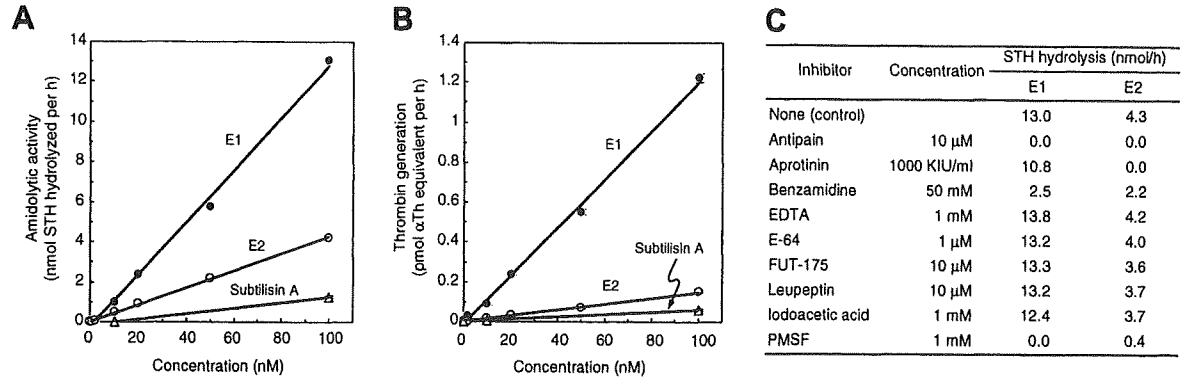

C

Inhibitor	Concentration	STH hydrolysis (nmol/h)	
		E1	E2
None (control)		13.0	4.3
Antipain	10 μM	0.0	0.0
Aprotinin	1000 KIU/ml	10.8	0.0
Benzamidine	50 mM	2.5	2.2
EDTA	1 mM	13.8	4.2
E-64	1 μM	13.2	4.0
FUT-175	10 μM	13.3	3.6
Leupeptin	10 μM	13.2	3.7
Iodoacetic acid	1 mM	12.4	3.7
PMSF	1 mM	0.0	0.4

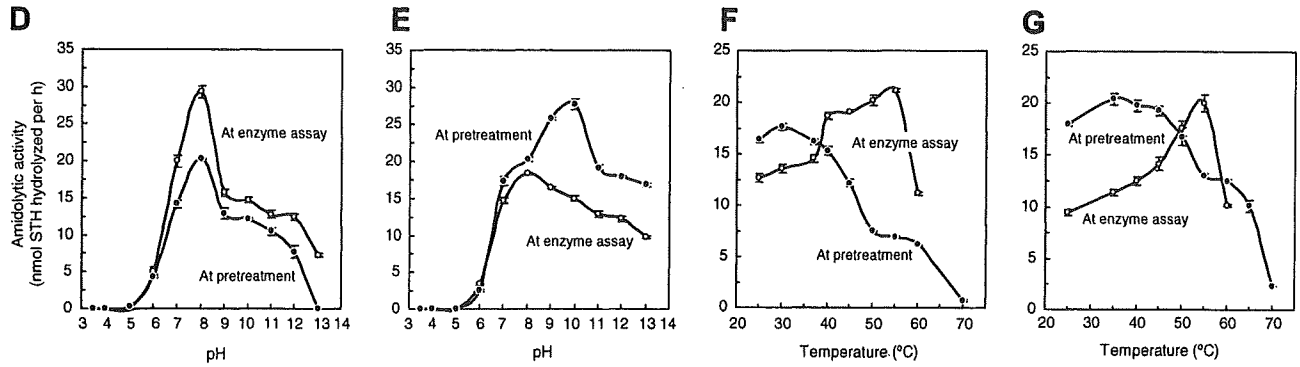

Fig. 2. Enzymatic properties of AS-E1 and -E2. Amidolytic activity toward Spectrozyme TH (A) and prothrombin activation promoting activity (B) were determined at the indicated concentrations of each enzyme. (C) The sensitivity of AS-E1 and -E2 to various inhibitors was examined by incubating each enzyme at 100 nM in the presence of the indicated substances under standard conditions using Spectrozyme TH as substrate. (D–G) The enzymatic activities of AS-E1 and -E2 were characterized using Spectrozyme TH as a substrate. (D,E) AS-E1 (100 nM) and AS-E2 (460 nM) were assayed for activity either at the indicated pH (○) or at pH 7.4 after preincubation at the indicated pH for 20 min at 25 °C (●). Buffers used were 200 mM sodium acetate (pH 3.5–5.6), 200 mM sodium phosphate (pH 5.8–8.0), and 100 mM glycine–NaOH (pH 9–13). (F,G) AS-E1 (100 nM) and AS-E2 (460 nM) were assayed for activity either at the indicated temperature (○) or at 25 °C after preincubation at the indicated temperature for 20 min at 25 °C in TBS/T/Ca (●). The concentration of AS-E1 and -E2 at pretreatment was 125 and 575 nM, respectively. Each value represents the mean ± SD from triplicate determinations.

EDTA, E-64, iodoacetic acid, leupeptin, and FUT-175 (6-amidino-2-naphthyl 4-guanidinobenzoate) showed only slight or no effects.

AS-E1 had optima at pH 8 and 55 °C (Fig. 2D and F). AS-E1 kept >50% of its activity after treatment at 25 °C for 20 min at pH 7–11, while the enzyme completely lost its activity by treatment at pH < 5 and 13 (Fig. 2D). When AS-E1 was treated at temperature above 40 °C for 20 min, the enzyme activity was reduced considerably, while the enzyme was stable at 25–40 °C (Fig. 2F). AS-E2 was similar to AS-E1 with respect to pH and temperature optima, whereas AS-E2 showed higher stability to high temperature and pH as compared with AS-E1 (Fig. 2E and G).

The above data suggest that both enzymes are alkaline serine proteases. These results are consistent with the observation that the sequences of AS-E1 and -E2 show significant similarity to sublilases, a broad family of subtilisin-like serine proteases [11].

Prothrombin cleavage

Both enzymes caused specific cleavages of prothrombin at relatively low concentrations (enzyme–substrate ratios of ~1:1000). When analyzed by nonreduced SDS–PAGE, the pattern of cleavage resembled that by factor Xa, an enzyme responsible to physiological activation of prothrombin (Fig. 3A). In spite of close similarities in apparent cleavage patterns, the major active molecular species generated by AS-E1 and -E2 were meizothrombin(desF1)-like molecules (molecular mass around 56 kDa) as judged from fibrinogen zymography (Fig. 3B). This result indicated that AS-E1 and -E2 cleaved prothrombin at sites distinct from those cleaved by Xa. Indeed, the analyses of the cleaved products on nonreduced SDS–PAGE demonstrated unique cleavages (Fig. 3C–G). Factor Xa cleaves prothrombin at Arg^{320}-Ile^{321} to afford meizothrombin as an intermediary thrombin species, which is subsequently cleaved at Arg^{271}-Thr^{272} to produce α-thrombin (Fig. 3C and I). The resulting thrombin cleaves Arg^{155}-Ser^{156} bond to yield the "byproducts" F1 and F2. AS-E1 seemed to cleave Arg^{155}-Ser^{156} first to afford fragments 1 and 3 (Fig. 3D, F, and I). This notion was supported by the observation that the addition of DAPA, a specific inhibitor of thrombin, did not affect the cleavage pattern (Fig. 3D, right panel). AS-E1 caused additional cleavages at Thr^{45}-Ala^{46}, Tyr^{316}-Ile^{317}, and an unidentified site in the protease domain, yielding the additional frag-

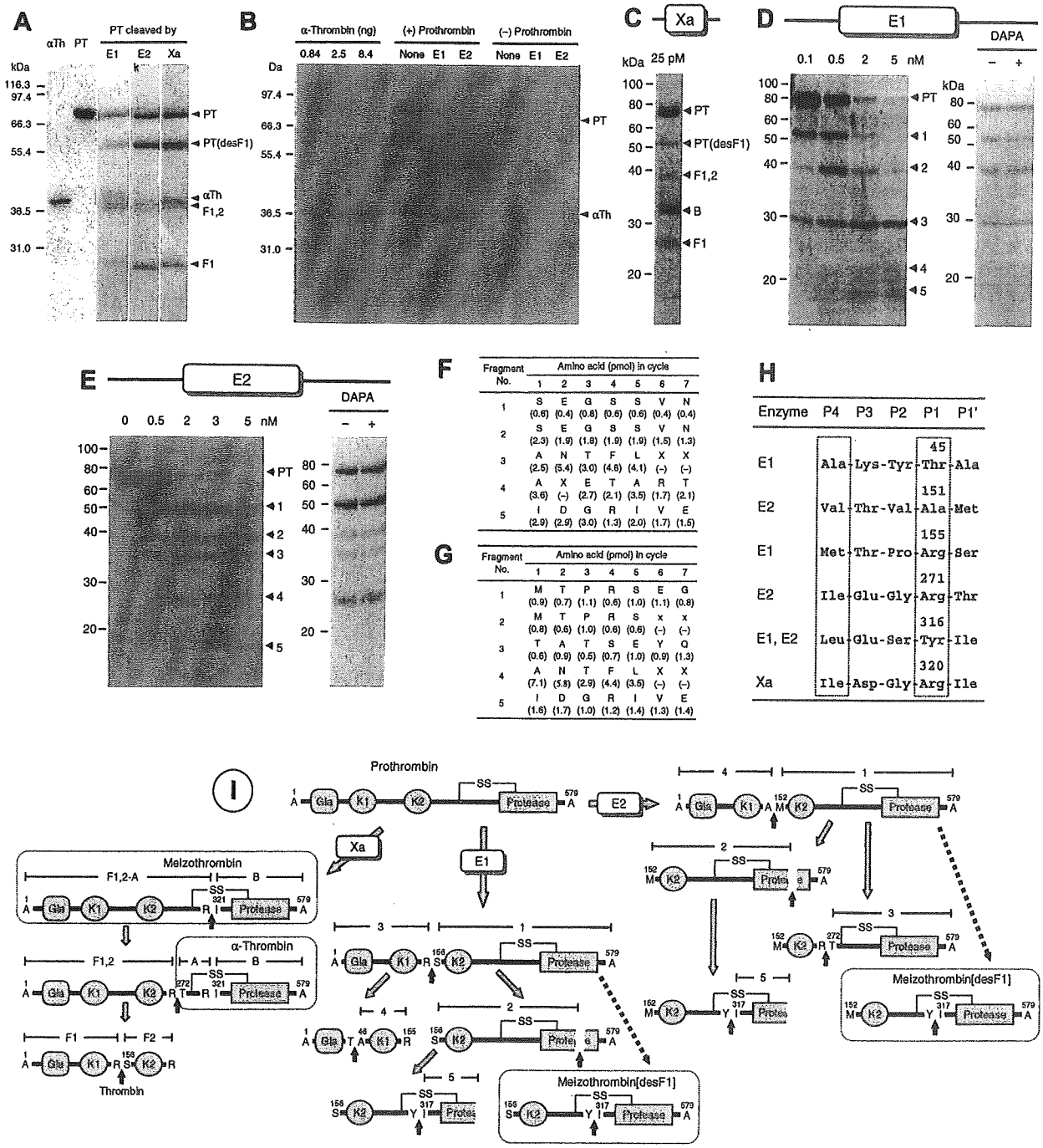

Fig. 3. Characterization of prothrombin cleavage by AS-E1 and -E2. (A) Prothrombin (2 μM) was incubated at 37 °C for 30 min with 2 nM AS-E1, 3 nM AS-E2 or 0.025 nM Xa with 0.1 nM Va and 50 μM phospholipids (prothrombinase complex), and aliquots were subjected to nonreduced SDS–PAGE. The positions of prothrombin (*PT*), α-thrombin (*αTh*), as well as prothrombin fragments generated by the Xa cleavage [prothrombin(desF1), F1,2 and F1] are shown. (B) Samples prepared as described in (A) were subjected to fibrinogen zymography. The amount of prothrombin degradation products applied to electrophoresis was 1.44 μg. As controls, no enzyme reaction mixture and reaction mixtures without prothrombin were also resolved. (C–E) Prothrombin that was incubated with enzymes as described in (A) was resolved on reduced SDS–PAGE. Where indicated, DAPA was included during the reaction. The positions of thrombin B-chain (given as B) and other fragments are shown. Prothrombin fragments generated by AS-E1 and -E2 are numbered. (F,G) N-terminal amino acid sequences of the numbered fragments are shown. (H) Amino acids near the sites cleaved by AS-E1 and -E2 are shown. (I) Possible structures of prothrombin fragments generated by cleavages with AS-E1 and -E2 as well as with Xa are shown schematically. *Solid line* represents a polypeptide chain. Domain structure is represented as a circle or a box: *Gla*, Gla domain; *K*, kringle domain; *protease*, serine protease domain. *Solid arrow* denotes cleavage site. *Dashed box* shows active enzyme species, while meizothrombin(desF1) is hypothetical.

ments 2, 4, and 5 (Fig. 3D). The cleavage site at Tyr^{316}-Ile^{317} is four residues proximal to the canonical Xa cleavage site (Arg^{320}-Ile^{321}). Although no fragment corresponding to thrombin B-chain was detected, we propose that the active molecular species generated by AS-E1-mediated prothrombin cleavage be a meizothrom-

bin(desF1)-like molecule with Ile^{317} as an N-terminus of B-chain (Fig. 3I) from the following notions. First, an activity migrates to a position similar to that of meizothrombin(desF1) on fibrinogen zymography (Fig. 3B). Second, a fragment with Ile^{317} as an N-terminus (fragment 5) can be found even after extensive degradations of prothrombin with high concentrations of AS-E1 (Fig. 3D), but any fragments starting with Ile^{321} are not found.

AS-E2 produced similar results as compared with those produced by AS-E1, while some positions of cleavage were different. The first cleavage seemed to occur at Ala^{151}-Met^{152} (instead of Arg^{155}-Ser^{156} by AS-E1), affording fragments 1 and 4. In addition, a unique cleavage at Arg^{271}-Thr^{272} to yield fragment 3 was observed (Fig. 3E, G, and I). These cleavages seemed to be due to AS-E2 activity itself because DAPA did not affect the proteolysis pattern (Fig. 3E, right panel). The AS-E2-mediated prothrombin activation products may also be the meizothrombin(desF1)-like molecule from similarity to the results obtained with AS-E1 (Fig. 3I).

Fig. 3H summarizes the positions of prothrombin cleavage by AS-E1 and -E2. Subtilisin, a canonical subtilase, recognizes hydrophobic and aromatic amino acids both at P1 and P4 [12]. On the other hand, kexins, which comprise the family E member of the subtilase superfamily, recognize Arg at P1. Kexins are characterized as that these have Asp^{166} at the bottom of the S1 pocket (instead of Gly^{166} in subtilisin) [11]. Thus, amino acid at position 166 in subtilases (the numbering is based on Ref. [11]) is important in determining specificity at P1. With respect to AS-E1 and -E2, amino acid at that position is predicted to be Tyr^{166} (residue 331 with symbol # in Supplementary Fig. 1). The two enzymes apparently recognized hydrophobic amino acids at P4, whereas their P1 recognition seemed to be less stringent, and they accepted even polar or basic residues at P1 (Fig. 3H).

Effects on plasma clotting

We asked whether AS-E1 and -E2 promote blood coagulation because the two enzymes directly activate prothrombin. We first tested their effects on clotting of human plasma using thrombelastography. AS-E1 and -E2 did not enhance but inhibit coagulation of plasma (Fig. 4A): no clot was formed at higher concentrations (>460 nM). When fibrinogen alone was used to monitor

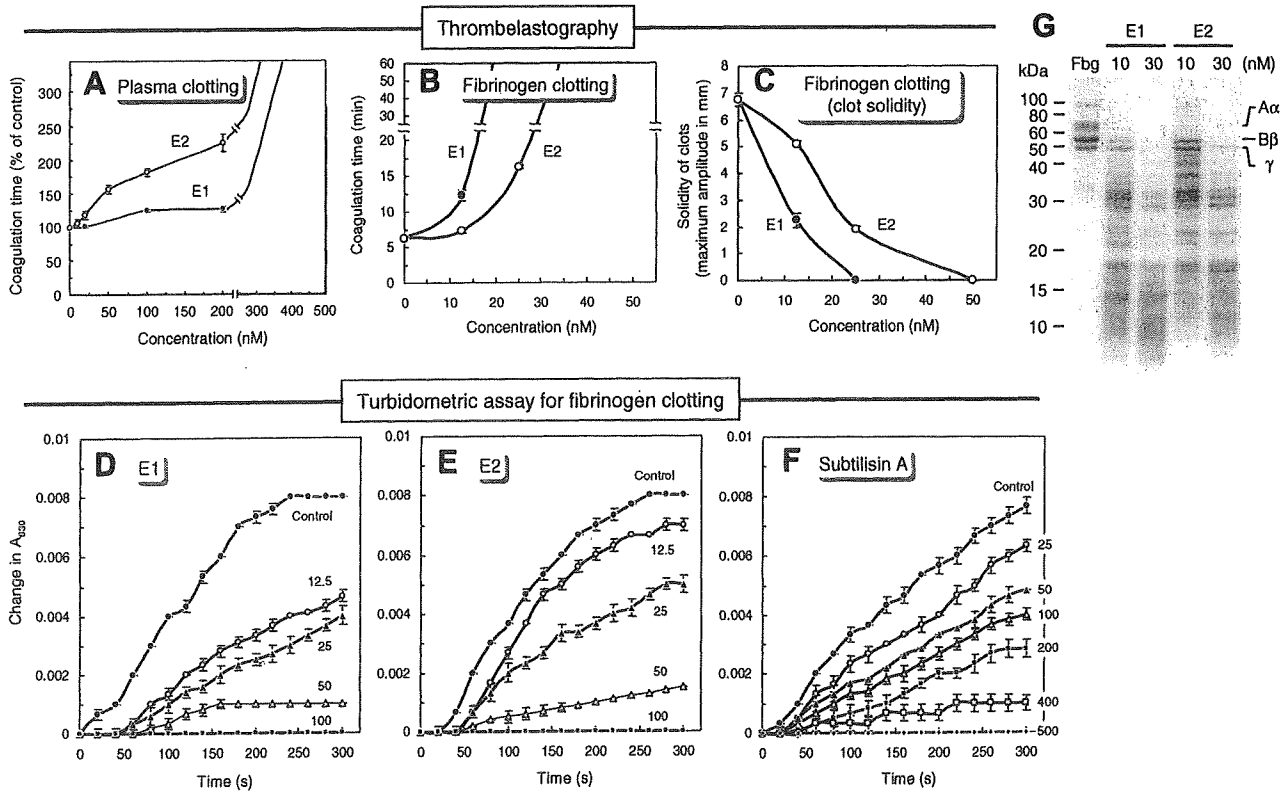

Fig. 4. Effects of AS-E1 and -E2 on the clotting of plasma and fibrinogen. (A) AS-E1 and -E2 at the indicated concentration was added to human plasma, and subjected to thrombelastography. Parameter shown is coagulation time (time required for the initiation of clot formation). Control coagulation time was 10.5 ± 2.5 min. (B,C) Thrombelastography was performed with fibrinogen after treatment with either AS-E1 or -E2 at the indicated concentrations. Coagulation time (B) and clot solidity (maximum amplitude) (C) are shown. Each value represents the average of duplicate determinations. (D–F) Fibrinogen clotting was measured by turbidometry after treatment with AS-E1 (D), AS-E2 (E) or subtilisin A (F) at the indicated concentrations (in nM). Each value represents the mean ± SD from triplicate determinations. (G) Patterns of fibrinogen degradation were examined after treatment with the indicated concentrations of AS-E1 or -E2 for 30 min at 60 °C, followed by reduced SDS–PAGE. The amount of degradation products applied was 10 μg, while the amount of fibrinogen standard (*Fbg*) was 2.5 μg. The positions of Aα, Bβ, and γ chains of fibrinogen are shown.

thrombin-induced coagulation, both enzymes also were inhibitory with respect to coagulation time and solidity of clots formed (Fig. 4B and C). The inhibition of coagulation was further confirmed by a turbidometric assay for fibrinogen clotting (Fig. 4D and E). Subtilisin A also inhibited fibrinogen clotting, although it was several times less potent than AS-E1 and -E2 (Fig. 4F). These results suggested that the inhibition of plasma clotting was in part due to degradation of fibrinogen. Indeed, fibrinogen was highly sensitive to degradation by AS-E1 and -E2, affording similar degradation products (Fig. 4G). Among the three subunits of fibrinogen, Aα chain appeared to be the most sensitive and was completely degraded by AS-E1 and -E2 at 10 nM (enzyme–substrate ratio at ~1:1400 by mol). Because the pattern of the fibrinogen cleavages was so complicated, we could not assign critical cleavage(s) responsible for the impairment of clotting.

The inhibition of plasma clotting by AS-E1 and -E2 can be explained as follows. Prothrombin and fibrinogen are similarly sensitive to cleavage by these enzymes (enzyme–substrate ratio at ~1:1000 is sufficient to specific cleavage), while the major product of prothrombin activation was meizothrombin(desF1)-like molecule. Meizothrombin(desF1) is far less potent than α-thrombin in causing fibrinogen clotting, but these are equally potent in activation of protein C (an anticoagulant zymogen) [13,14]. Thus, meizothrombin(desF1) may behave as an anticoagulant, rather than procoagulant. This notion is demonstrated with prothrombin Dhahran (R271H) and a recombinant mutant prothrombin R157A/R268A. These mutants are activated by Xa to generate a stable form of meizothrombin(desF1) or meizothrombin. Patients with prothrombin Dhahran display impaired blood coagulation [15], and prothrombin R157A/R268A inhibits experimental thrombosis [16]. Therefore, in addition to degradation of fibrinogen, the formation of meizothrombin(desF1)-like molecule may be the mechanism of the plasma clotting inhibition by AS-E1 and -E2.

Although the anticoagulant properties of these enzymes remain hypothetical under physiological conditions, these may play a role in part in tissue invasion of the microorganism in lesions affected by *Acremonium* and *Chaetomium* species, which cause onychomycosis (nail infection), peritonitis, corneal ulcers, and eumycotic mycetoma, as well as opportunistic infections in immunocompromised patients [17,18].

Appendix A. Supplementary data

Supplementary data associated with this article can be found, in the online version, at doi:10.1016/j.bbrc.2007.04.133.

References

[1] B. Furie, B.C. Furie, The molecular basis of blood coagulation, Cell 53 (1988) 505–518.
[2] J. Rosing, G. Tans, J.W. Govers-Riemslag, R.F. Zwaal, H.C. Hemker, The role of phospholipids and factor Va in the prothrombinase complex, J. Biol. Chem. 255 (1980) 274–283.
[3] J.W. Fenton II., Thrombin, Ann. N.Y. Acad. Sci. 485 (1986) 5–15.
[4] S.R. Coughlin, How the protease thrombin talks to cells, Proc. Natl. Acad. Sci. USA 96 (1999) 11023–11027.
[5] M. Levi, T. van der Poll, H. ten Cate, Tissue factor in infection and severe inflammation, Semin. Thromb. Hemost. 32 (2006) 33–39.
[6] R.M. Kini, The intriguing world of prothrombin activators from snake venom, Toxicon 45 (2005) 1133–1145.
[7] Z. Wegrzynowicz, P.B. Heczko, G.R. Drapeau, J. Jeljaszewicz, G. Pulverer, Prothrombin activation by a metalloprotease from *Staphylococcus aureus*, J. Clin. Microbiol. 12 (1980) 138–139.
[8] R. Narasaki, H. Kuribayashi, K. Shimizu, D. Imamura, T. Sato, K. Hasumi, M.A. Bacillolysin, A novel bacterial metalloproteinase that produces angiostatin-like fragments from plasminogen and activates protease zymogens in the coagulation and fibrinolysis systems, J. Biol. Chem. 280 (2005) 14278–14287.
[9] T. Imamura, A. Banbula, P.J. Pereira, J. Travis, J. Potempa, Activation of human prothrombin by arginine-specific cysteine proteinases (Gingipains R) from *Porphyromonas gingivalis*, J. Biol. Chem. 276 (2001) 18984–18991.
[10] N.J. Mutch, L.A. Robbie, N.A. Booth, Human thrombi contain an abundance of active thrombin, Thromb. Haemost. 86 (2001) 1028–1034.
[11] R.J. Siezen, J.A. Leunissen, Subtilases: the superfamily of subtilisin-like serine proteases, Protein Sci. 6 (1997) 501–523.
[12] J.J. Perona, C.S. Craik, Structural basis of substrate specificity in the serine proteases, Protein Sci. 4 (1995) 337–360.
[13] T.M. Hackeng, G. Tans, S.J. Koppelman, P.G. de Groot, J. Rosing, B.N. Bouma, Protein C activation on endothelial cells by prothrombin activation products generated in situ: meizothrombin is a better protein C activator than alpha-thrombin, Biochem. J. 319 (Pt. 2) (1996) 399–405.
[14] H.C. Côté, L. Bajzar, W.K. Stevens, J.A. Samis, J. Morser, R.T. MacGillivray, M.E. Nesheim, Functional characterization of recombinant human meizothrombin and meizothrombin(desF1), J. Biol. Chem. 272 (1997) 6194–6200.
[15] A.S. O'Marcaigh, W.L. Nichols, N.L. Hassinger, J.D. Mullins, A.A. Mallouh, G.S. Gilchrist, W.G. Owen, Genetic analysis and functional characterization of prothrombins Corpus Christi (Arg382-Cys), Dhahran (Arg271-His), and hypoprothrombinemia, Blood 88 (1996) 2611–2618.
[16] K. Shim, H. Zhu, L.A. Westfield, J.E. Sadler, A recombinant murine meizothrombin precursor, prothrombin R157A/R268A, inhibits thrombosis in a model of acute carotid artery injury, Blood 104 (2004) 415–419.
[17] A.K. Gupta, R.C. Summerbell, Combined distal and lateral subungual and white superficial onychomycosis in the toenails, J. Am. Acad. Dermatol. 41 (1999) 938–944.
[18] R.M. Fincher, J.F. Fisher, R.D. Lovell, C.L. Newman, A. Espinel-Ingroff, H.J. Shadomy, Infection due to the fungus *Acremonium* (*Cephalosporium*), Medicine (Baltimore) 70 (1991) 398–409.

Arch Dermatol Res (2007) 299:381–387
DOI 10.1007/s00403-007-0780-7

ORIGINAL PAPER

The effect of dermatophytes on cytokine production by human keratinocytes

Kenji Tani · Makoto Adachi · Yuka Nakamura · Rui Kano · Koichi Makimura · Atsuhiko Hasegawa · Naoko Kanda · Shinichi Watanabe

Received: 9 January 2007 / Revised: 2 July 2007 / Accepted: 2 August 2007 / Published online: 21 August 2007

Abstract Dermatophytosis (tinea) is a common disease in superficial mycoses and is generally confined to the stratum corneum in the epidermis and cutaneous appendages. The mechanisms by which dermatophytes cause dermatophytosis, however, are poorly understood. In this study, we evaluated the effect of *Trichophyton mentagrophytes*, *T. tonsurans* and *T. rubrum* on cytokine production by normal human epidermal keratinocytes (NHEKs). After 3–24 h of co-culture of NHEKs with each of the dermatophytes, cytokines in the supernatant were measured by enzyme-linked immunosorbent assay. Promoter activity of IL-8 was measured by chloramphenicol acetyl transferase (CAT) assay. IL-8 and GRO-α levels were higher in supernatants co-cultured with *T. mentagrophytes* isolates from animal than in those with *T. mentagrophytes* isolates from human, and with *T. tonsurans* and *T. rubrum* isolates. CAT expression for IL-8 promoter activity was higher in cell lysates stimulated with *T. mentagrophytes* isolates from animal than in those with *T. mentagrophytes* isolates from human, and with *T. tonsurans* and *T. rubrum* isolates. These findings suggest that dermatophytes directly induce production of cytokines at the transcriptional level by human keratinocytes, and that there are differences in their ability to induce cytokine production between the dermatophytes.

Keywords Cytokine · Dermatophyte · Dermatophytosis · Interleukin-8 · Keratinocyte

K. Tani · M. Adachi · Y. Nakamura · N. Kanda · S. Watanabe
Department of Dermatology,
Teikyo University School of Medicine,
2-11-1 Kaga, Itabashi-ku, Tokyo 173-8605, Japan

R. Kano · A. Hasegawa
Department of Pathobiology,
Nihon University School of Veterinary Medicine,
1866 Kameino, Fujisawa, Kanagawa 252-8510, Japan

K. Makimura
Teikyo University Institute of Medical Mycology,
539 Otsuka, Hachioji, Tokyo 192-0395, Japan

K. Tani (✉)
Department of Veterinary Surgery,
Faculty of Agriculture, Iwate University,
Ueda 3-18-8, Morioka 020-8550, Japan
e-mail: ktani@iwate-u.ac.jp

Introduction

Dermatophytosis is a common disease in superficial mycoses and is generally confined to the stratum corneum in the epidermis and cutaneous appendages [19]. The clinical features of dermatophytoses are determined by three factors: the particular species of fungus involved, the location of the infection and the host response [33]. The pathogens of dermatophytosis include *Trichophyton mentagrophytes*, *T. tonsurans*, T. *rubrum* and so on [19, 33]. Establishment of the phylogenetic classification of pathogenic fungi has been achieved by molecular biological studies [5, 6, 14, 16, 25, 29]. However, for dermatophytes, including *T. mentagrophytes*, the phylogenic relationship of species-specific sequences cannot be defined by these methods because the members of this group of fungi are phylogenetically and taxonomically very closely related. Recently, DNA sequence analysis of internal transcribed spacer 1 regions was established for closely related dermatophytes [20, 21, 24, 25]. This method could distinguish *T. mentagrophytes* complex, such as isolates from human and animal, as well as *Arthroderma vanbreuseghemii*, *A. benhamiae* and *A. simii* [20, 21]. Clinically, tinea corporis rather

than tinea unguium shows marked inflammatory reactions characterized by the infiltration of neutrophils but there are few mononuclear cells. In addition, the inflammation of the affected areas is often more severe in infections with *T. mentagrophytes* than with *T. rubrum* [33]. Zoophilic dermatophytes rather than anthropophilic dermatophytes are believed to induce severe inflammatory reactions [33]. However, the different mechanisms of dermatophytosis are poorly understood. Furthermore, a comparative study between *T. mentagrophytes* isolates from human and animal for their virulence has not been reported.

The physical and chemical structure of the skin represents a form of defense against these fungal pathogens. The epidermis of the skin is largely composed of keratinocytes, and they not only play an important structural part in forming a physical barrier to foreign microorganisms, but also are important functionally in mediating cutaneous immune reactions. We previously demonstrated that *T. mentagrophytes* induce interleukin (IL)-8 and tumor necrosis factor (TNF)-α production from keratinocytes [27]. In addition, other cytokines may regulate the immune response by keratinocytes. For example, granulocyte-macrophage colony stimulating factor (GM-CSF), produced by a variety cells including macrophages, endothelial cells, T cells and keratinocytes enhances growth promoting activity of granulocytes and also induces granulocyte and macrophage differentiation [10, 34]. GM-CSF is also important as a pleiotropic cytokine evoking complex processes during wound repair of the skin [11, 38]. Chemokines are a family of chemotactic cytokines, and they stimulate leukocyte movement [30]. In general, chemokine α family members, such as IL-8 and growth-related gene product (GRO)-α, preferentially chemoattract and activate neutrophils [4, 22], whereas chemokine β family members, such as regulated upon activation normal T expressed and secreted (RANTES) and monocyte chemotactic protein (MCP) -1, are chemotactic for T cells and monocytes [30, 36], respectively. These chemokines are also released from keratinocytes both in in vitro and in vivo situations [1–3, 17, 32].

In this study, we tested the hypotheses that dermatophytes (*T. mentagrophytes*, *T. tonsurans* and *T. rubrum*) induce cytokine production by human keratinocytes, and the different species are associated with different magnitudes of inflammatory cytokine responses by human keratinocytes.

Materials and methods

Fungal identification and cultures

Three isolates of *T. mentagrophytes* from animal and five isolates of *T. mentagrophytes*, two isolates of *T. rubrum* and two isolates of *T. tonsurans* were used in this study. All isolates were identified by conventional methods [15] and by specific DNA sequences of nuclear ribosomal internal transcribed spacer (ITS)1 regions as previously described [20, 21]. The sequences of the ITS1 regions of each isolates of *T. mentagrophytes*, *T. rubrum* and *T. tonsurans* were conformed to the data in National Center for Biotechnology Information data bank. The Genebank accession numbers were: *T. mentagrophytes* isolates from human, AB011463; *T. mentagrophytes* isolates from animal, AB011464; *T. rubrum*; AB011453; *T. tonsurans*; AB017172, respectively. The sequences of the three *T. mentagrophytes* isolates from animal were conformed to a sequence of *T. mentagrophytes* animal type 3 in ITS1 identical group described previously [20, 21]. All isolates were maintained by culturing at 25°C on 1/10 Sabouraud's dextrose agar (SDA) containing peptone 0.1%, dextrose 0.2%, KH_2PO_4 0.1%, $MgSO_47H_2O$ 0.1%, agar 2% and subcultured every 2 weeks more than two times before use.

Keratinocyte cultures

Normal human epidermal keratinocytes (NHEKs) were obtained as cryopreserved first passage cells from Clonetics (Bio Whittaker, San Diego, CA, USA). NHEKs were grown in 100 mm tissue culture dishes using the serum-free medium of keratinocyte-SFM (GIBCO BRL, Grand Island, NY, USA) supplemented with bovine pituitary extract (50 μg/ml) and human recombinant epidermal growth factor (2.5 ng/ml) at 37°C, 5% CO_2. The media was replaced every 2–3 days. When near confluence (70–90%), NHEKs were disaggregated using 0.025% trypsin/0.01% ethylenediamine tetraacetic acid in HEPES and subcultured. All experimental procedures were performed using second to fourth passage cells.

Co-culture of keratinocytes with dermatophytes

Co-culture of NHEKs with microconidia of *T. mentagrophytes*, *T. rubrum* and *T. tonsurans* was carried out based on a previous method [9]. Microconidia were collected by scraping from the colonies of *T. mentagrophytes*, *T. rubrum* and *T. tonsurans* grown on SDA and were suspended with phosphate buffered saline (PBS) containing 0.04% Tween 80 in a glass homogenizer. The suspension was filtered with a Whatman filter model 1 (pore size, 11 μm) to collect microconidia [35]. These microconidia were washed twice in PBS, and these were resuspended in basal medium. The human epidermal keratinocytes (1×10^5 cells/well) were incubated on a microplate with 24 wells at 37°C, 5% CO_2 for 12 h, and then the microconidia of each of the dermatophytes (final concentration, 2×10^5 cells/well) were added to the wells. Yeast cells of *Candida albicans* (final

concentration, 1×10^5 cells/well) were used as positive controls [13]. These supernatants were obtained after 3–24 h of co-culture and kept at −20°C until use for cytokine assay with ELISA.

Plasmid, transfection and chloramphenicol acetyl transferase (CAT) expression for IL-8 promoter activity

The fragment of the genomic IL-8 DNA, which spans nucleotides −1481 to +44 bp relative to the transcriptional start site, was subcloned into pCAT-basic vector (Promega, WI, USA) as described previously [12, 26]. Transfection of NHEKs was carried out by the poly-L-ornithine and dimethylsulfoxide (DMSO) shock method as described previously [28]. On the day of transfection, cells were washed and incubated in the basal medium without epidermal growth factor and pituitary extract. Each transfection contained 8 μg IL-8 promoter-CAT reporter and 2 μg pSV-β-Galactosidase Control Vector (Promega) in 60 mm dishes. Twenty-four hours after the DMSO shock, the medium was discarded and the cells were washed with phosphate-buffered saline, and incubated in basal medium without epidermal growth factor and pituitary extract in the presence or absence of 2×10^6 dermatophytes. After 24 h, the cells were harvested and lysed by three freeze/thaw cycles. The cell lysate was centrifuged, and supernatant was assayed for CAT expression by CAT-ELISA (Roche Diagnostics, Tokyo, Japan) and for β-Galactosidase expression by β-Gal ELISA (Roche Diagnostics) according to the manufacturer's instructions. Total protein amount was measured with a Bio-Rad protein assay kit. Interleukin-8 promoter activity was presented as a ratio of the CAT enzyme amount over the β-Galactosidase.

Co-culture of keratinocytes with dermatophytes on a polycarbonate filter

Human epidermal keratinocytes (1×10^5 cells/well) were incubated on a microplate with 24 wells, and then a polycarbonate filter (Transwell, 0.1 μm pore size, Corning, MA, USA) was mounted on the microplate. Dermatophytes (final concentration, 2×10^5 cells/well) suspended in keratinocyte-SFM without bovine pituitary extract and epidermal growth factor were added to the apical side of the filter. These supernatants were obtained after 3–24 h of co-culture and kept at −20°C until use for cytokine assay with ELISA.

Co-culture of keratinocytes with heat-killed dermatophytes

Microconidia of dermatophytes were killed under conditions of 56°C—30 min. No live colony was observed on Sabouraud's agar plate after the treatment. Co-cultures of NHEK with these heat-killed dermatophytes were carried out as described above. These supernatants were obtained after 3–24 h of co-culture and kept at −20°C until use for cytokine assay with ELISA.

Lactate dehydrogenase (LDH) assay

In order to evaluate dermatophyte-induced cytotoxicity of NHEKs, we performed LDH assay by use of a Cytotoxicity Detection kit (Roche Diagnostics) according to the manufacturer's instructions. LDH activity was determined by a coupled enzymic reaction whereby the tetrazolium salt was reduced to formazan. An increase in the number of dead or damaged cells resulted in an increase in LDH activity in the culture supernatant.

ELISA for cytokines

Cytoscreen Immunoassay kits (BioSource International, CA, USA) were used for IL-1β, IL-6, TNF-α, IL-8, MCP-1, RANTES and GM-CSF. A Quantikine kit was used for GRO-α (R&D System Inc. MN, USA). All ELISA kits were used according to the instruction manuals. The ELISA for cytokines was sensitive to ≥10 pg/ml.

Statistical analysis

All experiments were carried out in triplicate, and results are expressed as means ± SD. Comparisons between tests were done by the Student's t test, with statistical significance considered to be $P < 0.01$.

Results

Co-culture of keratinocytes with dermatophytes

Cytokine levels in the supernatants were determined by ELISA assay kit, after 3–24 h of co-culture of epidermal keratinocytes and dermatophytes. These results are shown in Fig. 1. IL-1β (Fig. 1a) and IL-6 (Fig. 1b) levels were low in each culture supernatant of keratinocytes with dermatophytes examined at every culturing time. TNF-α increased in the supernatant co-cultured with *T. mentagrophytes* only at 24 h after the culture (Fig. 1c). IL-8 and GRO-α were detected in the supernatant, and increased following co-culture with *T. mentagrophytes*, *T. tonsurans* and *T. rubrum* (Fig. 1d, e). IL-8 and GRO-α levels were higher in the supernatant co-cultured with *T. mentagrophytes* isolates from animal than in that with human isolates of *T. mentagrophytes*, *T. tonsurans* and *T. rubrum*. GM-CSF increased in the supernatant co-cultured with TM animal type only at

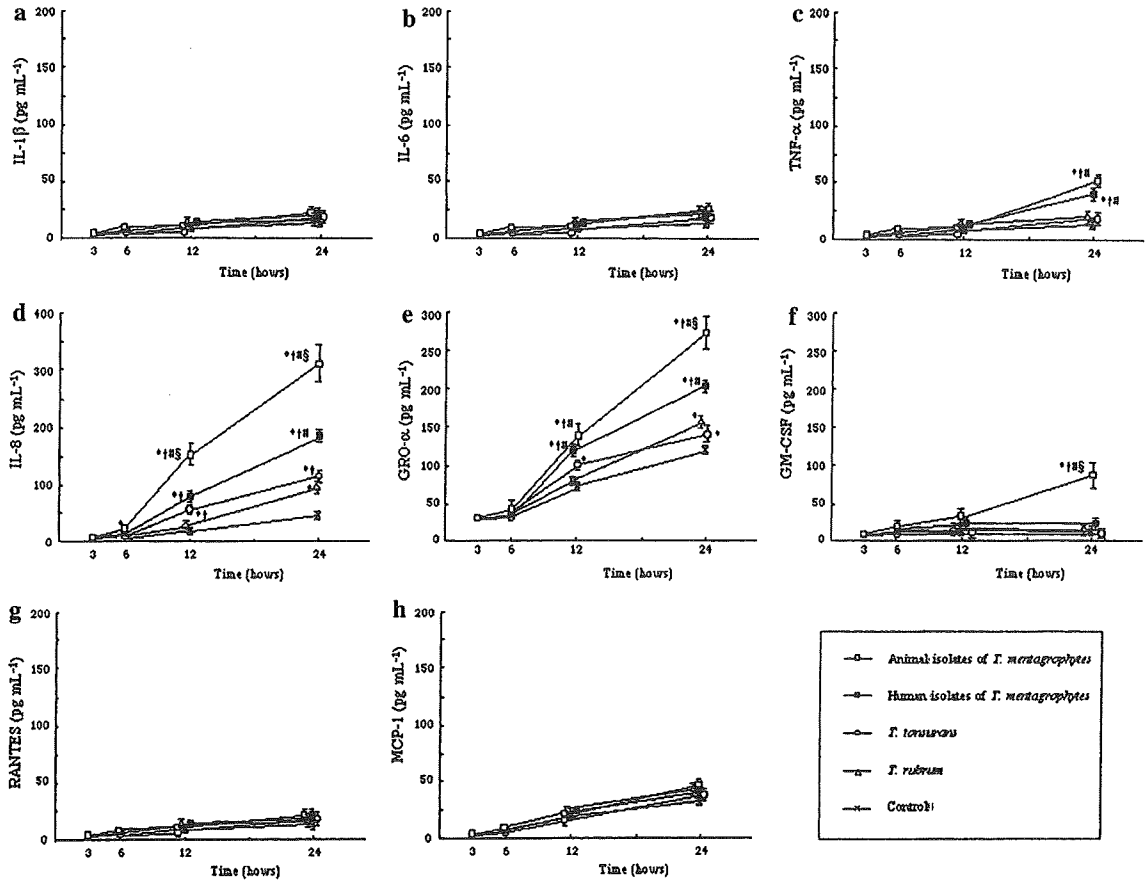

Fig. 1 Effect of dermatophytes on cytokine production by human keratinocytes. Keratinocytes were co-cultured with or without dermatophytes. After 3, 6, 12 and 24 h, cytokine levels (**a** IL-1β, **b** IL-6, **c** TNF-α, **d** IL-8, **e** GRO-α, **f** GM-CSF, **g** RANTES and **h** MCP-1) in the supernatant were measured by the ELISA method. Results are shown as representative data of three or four independent experiments. Data are mean ± SD. $*P < 0.01$ versus value without dermatophytes, $\dagger P < 0.01$ versus value with *T. rubrum*, $\#P < 0.01$ versus value with *T. tonsurans*, $\S P < 0.01$ versus value with *T. mentagrophytes* isolates from human

24 h after the culture (Fig. 1f). RANTES and MCP-1 levels were low, and there were no differences between each dermatophyte (Fig. 1g, h).

IL-8 promoter activity

Interleukin-8 promoter activity was presented as a ratio of the CAT enzyme amount over the β-Galactosidase amount. The CAT expression was higher in cell lysates co-cultured with *T. mentagrophytes* isolates from animal than in those with human isolates of *T. mentagrophytes*, *T. tonsurans* and *T. rubrum* (Fig. 2).

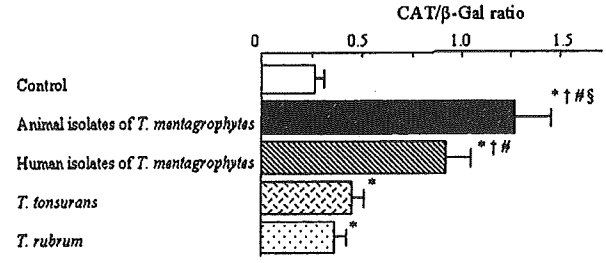

Fig. 2 IL-8 promoter activity. Interleukin-8 promoter activity was presented as a ratio of the CAT enzyme amount over the β-Galactosidase amount. Keratinocytes were transiently transfected with the 1481 bp IL-8 promoter-CAT reporter construct. After transfection, the cells were co-cultured with or without dermatophytes. Results are shown as representative data of four independent experiments. Data are mean ± SD. $*P < 0.01$ versus value without dermatophytes, $\dagger P < 0.01$ versus value with *T. rubrum*, $\#P < 0.01$ versus value with *T. tonsurans*, $\S P < 0.01$ versus value with *T. mentagrophytes* isolates from human

Co-culture of keratinocytes with dermatophytes on a polycarbonate filter

After 24 h of co-culture with each dermatophyte on a polycarbonate filter, IL-8 (Fig. 3a) and GRO-α (Fig. 3b) levels were low, and there were no significant differences between the groups with or without dermatophytes. IL-1β, IL-6, TNF-α, MCP-1, RANTES and GM-CSF levels were low, and there were no significant differences between the groups with or without dermatophytes (data not shown).

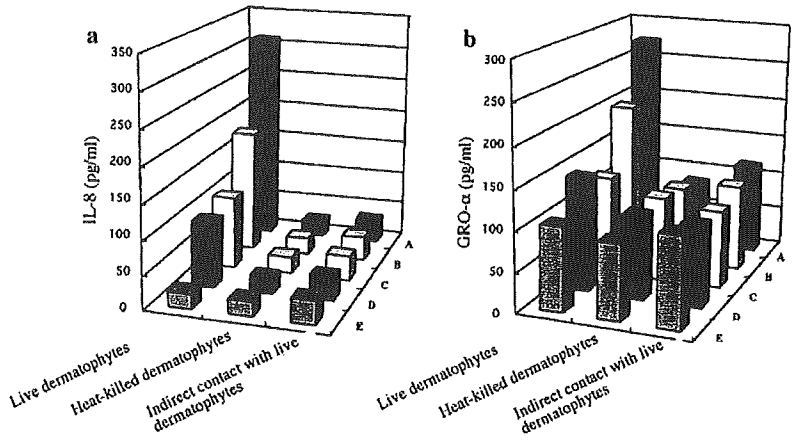

Fig. 3 Effect of heat-treatment and indirect contact on cytokine production by human keratinocytes. After 24 h of co-culture with each of the heat-killed dermatophytes and co-culture with dermatophytes on a polycarbonate filter (0.1 μm pore size), IL-8 (**a**) and GRO-α (**b**) levels were measured by the ELISA method. Results are shown as representative data of four independent experiments. *A T. mentagrophytes* isolates from animal, *B T. mentagrophytes* isolates from human, *C T. tonsurans*, *D T. rubrum*

Co-culture of keratinocytes with heat-killed dermatophytes

After 24 h of co-culture with each of the heat-killed dermatophytes, IL-8 (Fig. 3a) and GRO-α (Fig. 3b) levels were low and there were no significant differences between the groups with or without dermatophytes. IL-1β, IL-6, TNF-α, MCP-1, RANTES and GM-CSF levels were low, and there were no significant differences between the groups with or without dermatophytes (data not shown).

Cell viability

The release of cytokines was not due to cell lysis. LDH, which is a cytoplasmic marker, was found to be present in the supernatant of co-cultures with or without dermatophyte stimuli. Overall, growth and viability of NHEKs remained viable throughout the 24 h co-culture period.

Discussion

In this study, we demonstrated that causative dermatophytes could induce cytokine production by NHEKs at transcriptional levels, and that there were differences in their ability to induce the cytokine production by NHEKs between dermatophytes. These differences in ability to induce cytokine production may reflect different inflammatory responses, which in turn may reflect the capacity of NHEKs to detect virulence activities of dermatophytes. Cytokine production was strongly enhanced during the co-culturing with *T. mentagrophytes*, whereas lower levels were seen with *T. tonsurans* and *T. rubrum*. In addition, *T. mentagrophytes* isolates from animal induced cytokine production by NHEKs more strongly than *T. mentagrophytes* isolates from human. These results support the finding that the inflammation of the affected areas is often more severe in infections with *T. mentagrophytes* than with *T. rubrum* and that zoophilic dermatophytes induce severe inflammatory reactions rather than anthropophilic dermatophytes [33]. The differences observed in cytokine production might partly due to differences in their growth rate in the media used for co-culture. However, similar cytokine expression by keratinocytes in different virulence of *Malassezia* yeasts [39] and *Candida* species [37] has been described. Thus, NHEKs are functionally important in mediating cutaneous immune reactions against dermatophytes.

Dermatophytes described in this study induced IL-8 and GRO-α production from NHEKs, although TNF-α and GM-CSF were also released from NHEKs co-cultured only with *T. mentagrophytes*. IL-1β, IL-6 and RANTES were not related to the effect of any of the dermatophytes in our system. These results suggest that dermatophytes induce chemokines such as IL-8 and GRO-α more than inflammatory cytokines such as IL-1β, IL-6 and TNF-α production from NHEKs. Interestingly, MCP-1 was not related to the effect of any of the dermatophytes. Therefore, NHEKs stimulated with dermatophytes play an important role as chemoattractants and activation for neutrophils but not for monocyte recruitment, although other chemoattractant molecules released from NHEKs could be involved in monocyte recruitment. These results correspond to the histopathologic features of dermatophytosis characterized by the infiltration of neutrophils but there are few mononuclear cells within parakeratotic foci in the dermis. In experimental dermatophytosis

using the mouse model, infiltrating cells are neutrophils, and monocytes do not appear until the chronic phase [7]. Thus, elongation of the co-culture period may induce MCP-1 production from keratinocytes. In this study, GM-CSF increased only at 24 h after being co-cultured with TM animal type. GM-CSF enhances neutrophil antifungal activity by oxidative metabolism and release of lysozymes and chemotactic factors [18, 23]. An increase of GM-CSF in keratinocytes stimulated with TM animal type isolates also may support those zoophilic dermatophytes rather than anthropophilic dermatophytes that induce severe inflammatory reactions.

Heat-killed dermatophytes cannot induce cytokine production by NHEKs. In contrast, both live and heat-killed bacteria can induce cytokine production [31]. This suggests that not only simply fungal surface molecules but also factors actively produced or modified by dermatophytes are crucial for the stimulation of cytokine expression. Furthermore, a polycarbonate filter prevented dermatophytes from inducing cytokine production by NHEKs in this study. These results suggest that causative dermatophytes may not release a soluble factor to stimulate cytokine production by NHEKs and that cell-to-cell contact between dermatophytes and NHEKs plays an important part in cytokine production. It is also possible that a soluble factor is released by the dermatophytes once they establish contact with keratinocytes. The data in this study suggest that the thickness of the horny layer is important for determining the clinical features of dermatophytoses because a frequency of cell-to-cell contact between dermatophytes and keratinocytes may depend upon the thickness. A recent study has suggested the importance of hydrolytic enzymes for the virulence of *C. albicans*, which is a pathogen of superficial mycoses [8]. Since heat-treatment degenerates proteins such as enzymes, it seems reasonable for these enzymes to be associated with the virulence of fungal diseases. However, there has been no report concerning the virulence factors of dermatophytes. Further investigations are needed to study the interaction of these fungal virulence factors and the immune response of the host.

In conclusion, keratinocytes not only form a physical barrier to dermatophytes but also mediate cutaneous immune reactions. Causative dermatophytes could release cytokines, particularly chemokines such as IL-8 and GRO-α, which chemoattract and activate neutrophils. There are the differences between the dermatophytes in their ability to induce cytokine production in keratinocytes. We also conclude that the cell-to-cell contact between dermatophytes and keratinocytes plays an important role in cytokine production by human keratinocytes.

Acknowledgments This work was supported by the Japan Health Sciences Foundation.

References

1. Albanesi C, Scarponi C, Sebastiani S, Cavani A, Federici M, Sozzani S, Girolomoni G (2001) A cytokine-to-chemokine axis between T lymphocytes and keratinocytes can favor Th1 cell accumulation in chronic inflammatory skin diseases. J Leukoc Biol 70:617–623
2. Ansel J, Perry P, Brown J, Damm D, Phan T, Hart C, Luger T, Hefeneider S (1990) Cytokine modulation of keratinocyte cytokines. J Invest Dermatol 94:101S–107S
3. Anttila HS, Reitamo S, Erkko P, Ceska M, Moser B, Baggiolini M (1992) Interleukin-8 immunoreactivity in the skin of healthy subjects and patients with palmoplantar pustulosis and psoriasis. J Invest Dermatol 98:96–101
4. Baggiolini M, Walz A, Kunkel SL (1989) Neutrophil-activating peptide-1/interleukin 8, a novel cytokine that activates neutrophils. J Clin Invest 84:1045–1049
5. Davison FD, Mackenzie DW (1984) DNA homology studies in the taxonomy of dermatophytes. Sabouraudia 22:117–123
6. Harmsen D, Schwinn A, Weig M, Brocker EB, Heesemann J (1995) Phylogeny and dating of some pathogenic keratinophilic fungi using small subunit ribosomal RNA. J Med Vet Mycol 33:299–303
7. Hay RJ, Calderon RA, Mackenzie CD (1988) Experimental dermatophytosis in mice: correlation between light and electron microscopic changes in primary, secondary and chronic infections. Br J Exp Pathol 69:703–716
8. Hube B, Naglik J (2001) *Candida albicans* proteinases: resolving the mystery of a gene family. Microbiology 147:1997–2005
9. Jiang Y, Russell TR, Graves DT, Cheng H, Nong SH, Levitz SM (1996) Monocyte chemoattractant protein 1 and interleukin-8 production in mononuclear cells stimulated by oral microorganisms. Infect Immun 64:4450–4455
10. Jones TC (1994) Future uses of granulocyte-macrophage colony-stimulating factor (GM-CSF). Stem Cells 12(Suppl 1):229–239; discussion 239–240
11. Jyung RW, Wu L, Pierce GF, Mustoe TA (1994) Granulocyte-macrophage colony-stimulating factor and granulocyte colony-stimulating factor: differential action on incisional wound healing. Surgery 115:325–334
12. Kanda N, Nakai K, Watanabe S (2001) Gangliosides GD1b, GT1b, and GQ1b suppress the growth of human melanoma by inhibiting interleukin-8 production: the inhibition of adenylate cyclase. J Invest Dermatol 117:284–293
13. Kano R, Hasegawa A, Watanabe S, Sato H, Nakamura Y (2003) *Candida albicans* induced interleukin 8 production by human keratinocytes. J Dermatol Sci 31:233–235
14. Kawasaki M, Aoki M, Ishizaki H, Nishio K, Mochizuki T, Watanabe S (1992) Phylogenetic relationships of the genera Arthroderma and Nannizzia inferred from mitochondrial DNA analysis. Mycopathologia 118:95–102
15. Kwon-Chung KJ, Bennett JE (1992) Medical mycology. Lea & Febiger, Philadelphia
16. Leclerc MC, Philippe H, Gueho E (1994) Phylogeny of dermatophytes and dimorphic fungi based on large subunit ribosomal RNA sequence comparisons. J Med Vet Mycol 32:331–341
17. Li J, Farthing PM, Thornhill MH (2000) Oral and skin keratinocytes are stimulated to secrete monocyte chemoattractant protein-1 by tumour necrosis factor-alpha and interferon-gamma. J Oral Pathol Med 29:438–444

18. Liehl E, Hildebrandt J, Lam C, Mayer P (1994) Prediction of the role of granulocyte-macrophage colony-stimulating factor in animals and man from in vitro results. Eur J Clin Microbiol Infect Dis 13(Suppl 2):S9–S17
19. Longley BJ (1997) Lever's histopathology of the skin, 8th edn. Lippincott-Raven, Philadelphia
20. Makimura K, Mochizuki T, Hasegawa A, Uchida K, Saito H, Yamaguchi H (1998) Phylogenetic classification of *Trichophyton mentagrophytes* complex isolates based on DNA sequences of nuclear ribosomal internal transcribed spacer 1 regions. J Clin Microbiol 36:2629–2633
21. Makimura K, Tamura Y, Mochizuki T, Hasegawa A, Tajiri Y, Hanazawa R, Uchida K, Saito H, Yamaguchi H (1999) Phylogenetic classification and species identification of dermatophyte isolates based on DNA sequences of nuclear ribosomal internal transcribed spacer 1 regions. J Clin Microbiol 37:920–924
22. Matsushima K, Larsen CG, DuBois GC, Oppenheim JJ (1989) Purification and characterization of a novel monocyte chemotactic and activating factor produced by a human myelomonocytic cell line. J Exp Med 169:1485–1490
23. Mayer P, Schutze E, Lam C, Kricek F, Liehl E (1991) Recombinant murine granulocyte-macrophage colony-stimulating factor augments neutrophil recovery and enhances resistance to infections in myelosuppressed mice. J Infect Dis 163:584–590
24. Mochizuki T, Kawasaki M, Ishizaki H, Makimura K (1999) Identification of several clinical isolates of dermatophytes based on the nucleotide sequence of internal transcribed spacer 1 (ITS 1) in nuclear ribosomal DNA. J Dermatol 26:276–281
25. Mochizuki T, Takada K, Watanabe S, Kawasaki M, Ishizaki H (1990) Taxonomy of Trichophyton interdigitale (*Trichophyton mentagrophytes* var. interdigitale) by restriction enzyme analysis of mitochondrial DNA. J Med Vet Mycol 28:191–196
26. Mukaida N, Shiroo M, Matsushima K (1989) Genomic structure of the human monocyte-derived neutrophil chemotactic factor IL-8. J Immunol 143:1366–1371
27. Nakamura Y, Kano R, Hasegawa A, Watanabe S (2002) Interleukin-8 and tumor necrosis factor alpha production in human epidermal keratinocytes induced by *Trichophyton mentagrophytes*. Clin Diagn Lab Immunol 9:935–937
28. Nead MA, McCance DJ (1995) Poly-L-ornithine-mediated transfection of human keratinocytes. J Invest Dermatol 105:668–671
29. Nishio K, Kawasaki M, Ishizaki H (1992) Phylogeny of the genera Trichophyton using mitochondrial DNA analysis. Mycopathologia 117:127–132
30. Oppenheim JJ, Zachariae CO, Mukaida N, Matsushima K (1991) Properties of the novel proinflammatory supergene "intercrine" cytokine family. Annu Rev Immunol 9:617–648
31. Paludan SR (2000) Synergistic action of pro-inflammatory agents: cellular and molecular aspects. J Leukoc Biol 67:18–25
32. Raychaudhuri SP, Jiang WY, Farber EM, Schall TJ, Ruff MR, Pert CB (1999) Upregulation of RANTES in psoriatic keratinocytes: a possible pathogenic mechanism for psoriasis. Acta Derm Venereol 79:9–11
33. Roscoe J, Farmer ER (2000) Pathology of the skin, 2nd edn. McGraw-Hill, New York
34. Ruef C, Coleman DL (1990) Granulocyte-macrophage colony-stimulating factor: pleiotropic cytokine with potential clinical usefulness. Rev Infect Dis 12:41–62
35. Santos DA, Hamdan JS (2005) Evaluation of broth microdilution antifungal susceptibility testing conditions for *Trichophyton rubrum*. J Clin Microbiol 43:1917–1920
36. Schall TJ (1991) Biology of the RANTES/SIS cytokine family. Cytokine 3:165–183
37. Schaller M, Mailhammer R, Grassl G, Sander CA, Hube B, Korting HC (2002) Infection of human oral epithelia with Candida species induces cytokine expression correlated to the degree of virulence. J Invest Dermatol 118:652–657
38. Vyalov S, Desmouliere A, Gabbiani G (1993) GM-CSF-induced granulation tissue formation: relationships between macrophage and myofibroblast accumulation. Virchows Arch B Cell Pathol Incl Mol Pathol 63:231–239
39. Watanabe S, Kano R, Sato H, Nakamura Y, Hasegawa A (2001) The effects of Malassezia yeasts on cytokine production by human keratinocytes. J Invest Dermatol 116:769–773

Int. J. Environ. Sci. Tech., 4 (2): 241-246, 2007
ISSN: 1735-1472

Evaluation of QIAamp DNA mini kit for removing of inhibitors in detection of *Cryptosporidium parvum* oocysts in water samples by a nested– PCR assay

[1*]*M. Nikaeen;* [2]*K. Makimura*

[1]*Department of Environmental Health Engineering, School of Public Health, Isfahan University of Medical Sciences, Isfahan, Iran*

[2]*Department of Molecular Biology and Gene Diagnosis, Teikyo University, Tokyo, Japan*

Received 29 November 2006; revised 26 February 2007; accepted 5 March 2007; available online 20 March 2007

ABSTRACT: In recent years, there has been a dramatic increase in the occurrence of waterborne disease outbreaks caused by the *Cryptosporidium parvum*, and presence of this protozoan parasite in drinking water is a significant health problem faced by the water industry. A new strategy for detection of *Cryptosporidium* oocysts in water samples is polymerase chain reactor based techniques. In this study a nested–PCR assay was designed for the specific amplification of a 199 bp DNA fragment of the gene encoding the heat shock protein (hsp 70) of *Cryptosporidium parvum* oocysts. In order to prevent the inhibition of PCR amplification by substances contained in water samples, three DNA purification methods including QIAamp DNA mini kit, InstaGene Matrix, MagExtractor – Genome were compared in concentrates of tap water samples spiked with the oocysts. After it was found that the QIAamp is only efficient purification technique, the efficiency of QIAamp and immunomagnetic separation for nested–PCR assay of various water samples was compared. The results show that QIAamp provide a useful and rapid tool for removing of PCR inhibitors. It seems that QIAamp purification- nested PCR assay is a sensitive, rapid and cost effective method for detection of *Cryptosporidium parvum* oocysts in clean water samples with turbidity < 2 nephelometric turbidity unit.

Key words: *Cryptosporidium, polymerase chain reactor, detection, QIAamp, water, purification*

INTRODUCTION

The protozoan parasite *Cryptosporidium parvum* has recently been recognized as an important cause of waterborne gastrointestinal disease worldwide (Fayer, *et al.*, 2000; Sturbaum, *et al.*, 2002). The organism can cause self-limited diarrhea in immunocompetent hosts and chronic, life threatening diarrhea in immunocompromised individuals, such as patients receiving immunosuppressive therapy and those suffered from acquired immunodeficiency syndrome (AIDS) (Fayer and Ungar, 1986).

The widespread occurrence of *Cryptosporidium* oocysts in surface waters (LeChevallier and Norton, 1995; LeChevallier, *et al.*, 1991; Lisle and Rose, 1995), the low dosage required for infection (Dupont, *et al.*, 1995) and their resistance to the normal chlorine disinfection level used in water treatment plants (Korich, *et al.*, 1990) has become a major concern for water industry and increased the need for understanding occurrence and distribution of the parasite in drinking and environmental waters. Therefore effective monitoring methods required for detection of *Cryptosporidium* oocysts in water samples. The immunofluorescence assay (IFA) which is widely used for detection of *Cryptosporidium* oocysts in water samples has many limitations (LeChevallier, *et al.*, 2003). Considerable effort is being made worldwide to improve detection methodologies through the application of techniques such as flow cytometry (Vesey, *et al.*, 1994) ELISA (De La Cruz and Sivaganesan, 1994) and polymerase chain reactor (PCR) (Johnson, *et al.*, 1995; Kozwich, *et al.*, 2000; Mayer and Palmer, 1996; Rochelle, *et al.*, 1997a). PCR in particular is a rapid, sensitive and pathogen specific (Kauncer and Stinear, 1998; Rochelle, *et al.*, 1997a) procedure that can overcome the limitations of other methods. PCR amplification enabled detection of one *Cryptosporidium* oocyst in purified samples, but the method faces some limitations in testing of water

*Corresponding author, Email: *nikaeen_m@yahoo.com*
Tel.: +98 311 7922 660; Fax:+98 311 6682 509

inhibitors such as humic acids (Johnson, *et al.*, 1995; Lowery, *et al.*, 2000; Rochelle, *et al.*, 1997a). Attempts have been made to overcome this problem by purification of extracted nucleic acids by spin column (Rochelle, *et al.*, 1997b), addition of compounds to amplification reaction mixtures to overcome inhibition (Rochelle, *et al.*, 1997a), hybridization to specific probes (Awad-el-Kariem, *et al.*, 1994; Carraway, *et al.*, 1996) and immunomagnetic separation (IMS) of target microbial pathogens before DNA extraction (Deng, *et al.*, 1997; Griffin and Rose, 1995; Hallier-Soulier and Guillot, 1999). In the present study firstly we evaluate efficiency of three DNA purification methods including QIAamp DNA mini kit, Instagene Matrix and MagExtractor Genome for detection of *Cryptosporidium parvum* oocysts spiked in packed pellet concentrates of tap water by a nested-PCR assay. We compared IMS–nested PCR and QIAamp–nested PCR for detection of low numbers of *C.Parvum* oocysts seeded in various concentrated water samples.

MATERIALS AND METHODS

C.Parvum oocysts stock: *Cryptosporidium parvum* oocysts were obtained as purified and enumerated form from National Institute of Infectious Diseases (NIID, Tokyo, Japan). Different oocyst densities were prepared by dilution in sterile deionized water. Nested-PCR sensitivity evaluation: sensitivity of nested-PCR was tested with different numbers of purified *C. Parvum* oocysts. Spiking of test water samples: in order to evaluate the performance of the purification methods, packed pellets of tap water samples (50 L) spiked with 100 *Cryptosporidium* oocysts in triplicate for each method. Packed pellets of water samples were obtained by filtering of water through a 142 mm diameter cellulose nitrate membrane filter (Millipore) with a pore size of 1.2 μm. After filtration, the membrane was carefully rinsed with phosphate buffered saline (PBS) containing 0.02 % sodium dodecyle sulfate (SDS) and tween 80 and centrifuged for 15 min at 3000 rpm to produce packed pellet. Extraction of nucleic acid: DNA was extracted from purified oocysts by eight cycles of freezing in liquid nitrogen for 1 min, followed by thawing at 98 °C for 1 min.

DNA extraction and purification of spiked concentrates:

Instagen Matrix (Bio-Rad): DNA was released in the presence of Instagen Matrix by eight cycles of freezing and thawing. DNA was then removed by centrifugation for 3 min at 12000 rpm and used directly in PCR reaction.

MagExtractor – Genome (Toyobo): according to the manufacturer's protocol 750 μL lysis buffer and 40 μL of magnetic beads were added to pellets containing oocysts. After eight cycles of freeze and thaw, DNA purification was performed as outlined by the manufacture.

QIAamp DNA min kit (QIAgen K.K., Japan): DNA was extracted and purified from spiked concentrates of water samples by using a QIAamp DNA min kit according to the manufacturer's instruction with some modifications including eight cycles of freeze and thaw after incubation at 56 °C and rapid centrifugation before purification of DNA by spin columns.

PCR: A nested–PCR was performed to detect *Cryptosporidium* oocysts. PCR primers (CPHSP2) which amplified a 361 bp fragment of *C. parvum* heat shock protein gene (hsp70) were reported previously by Rochelle, *et al.* (1997b). Nested primers NesCPHF (5μ- TGGTGGTGTTATGACCAAGC) and NesCPHR (5μ-TGGTACACCTCTTGGTGCT G) which amplified a 199 bp product within the first amplicon were designed using DNASIS software (Hitachi software, Japan). The reaction was carried out on a PCR thermal cycler (Takara, Japan) in 200 μL PCR tubes containing 30 μL of reaction mixture and 20μL of template. The primary PCR contained 100 μM dNTP, 300 nM each forward and reverse CPHSP2 primers, 2.5 μLof bovine serum albumin (10 mg/mL, sigma), 1× PCR buffer, 1.25 unit of *taq* polymerase. The nested PCR amplified 1 μL of the primary PCR product. The secondary PCR components were the same as the primary PCR with the exception of nested primers and concentration of dNTP (20 μM). Bovine serum albumin also was not included in the reaction mixture.

The following thermal protocol was used: primary PCR consisted of an initial denaturation at 95 °C for 5 min; 35 cycles of 94 °C for 1 min, 55 °C for 2 min and 72 °C for 1 min and final extension at 72 °C for 10 min. The nested PCR amplification parameters were 5 min at 94 °C, 30 s at 94 °C, 45 s at 58 °C, and 30 s at 72 °C for 30 cycles; and finally 10 min at 72 °C.

Positive and negative controls were run with every PCR set. Detection of amplified PCR products: The PCR product was analyzed by electrophoresis in a 1.6% ogarose gel and was visualized with a image master VDS system (Pharmacia, Biotech) after staining with etidium bromide (0.5 μg/mL).

Comparison between QIAamp–nested PCR and IMS–nested PCR: replicate tubes containing different water sample concentrates which spiked with *C.Parvum* oocysts were processed by both QIAamp–nested PCR and immunomagnetic separation (IMS)-nested PCR. The turbidity of water samples was determined with a spectrophotometer (BEKMAN DU 650). Immunomagnetic separation: spiked concentrates of water samples were subjected to IMS as outlined by manufacture and then purified oocycts subjected to the DNA extraction by eight cycles of freeze and thaw. Negative control in which oocyst or DNA was replaced with sterile distilled water were included in the spiking step and in the PCR amplification.

RESULTS

Nested – PCR assay sensitivity: to determine the sensitivity of newly designed nested–PCR primer set described in this study, dilution of *C. Parvum* oocysts were prepared and nested–PCR was performed. Fig. 1 a shows that with CPHSP primers, oocyst dilutions were detected at a level of approximately 10^2 oocysts, but using nested -PCR it can detect as few as one oocyst (Fig. 1b). Efficiency of purification methods: nested–PCR amplification of the DNA purified by QIAamp from the tap water concentrates seeded with 10^2 *Cryptosporidium* oocysts generated a 199 bp DNA fragment. However when other DNA purification methods were used with the tap water concentrates, which were seeded similarly with *Cryptosporidium* oocysts, the target gene failed to amplify.

These results suggest that other DNA purification procedures except QIAamp may not yield enough pure DNA to support PCR amplification for detection of *Cryptosporidium* oocysts in tap water.

Limit of detection of QIAamp-nested PCR: To demonstrate the sensitivity of the method, the limit of the detection when QIAamp used as DNA purification procedure was determined by spiking of tap water concentrates with 10, 5 and 1 oocyst. Fig. 2 shows that nested–PCR could amplify as few as one oocyst spiked in packed pellet concentrates of 50 liters tap water. Comparison of IMS–nested PCR and QIAamp–nested PCR: A comparative study between the IMS-nested PCR assay and QIAamp-nested PCR was carried out on spiked concentrates of treated and untreated water samples. The results are summarized in table 1. These results show that our extraction purification method is compatible with low turbidity environmental water samples and the discrepancy between the two methods is related to environmental water samples with turbidities higher than 2 NTU.

DISCUSSION AND CONCLUSION

A common problem in PCR amplification of DNA extracted from environmental samples is inhibition by humic type materials that co-extract with DNA (Kozwich, *et al.*, 2000; Mahbubani, *et al.*, 1998). Techniques used specifically to relieve the inhibition and enhance PCR detection of *Cryptosporidium* oocysts include flow cytometry and immunomagnetic separation of oocysts from water samples prior to PCR (Johnson et al., 1995), and spin column purification of extracted DNA (Rochelle, *et al.*, 1997b).

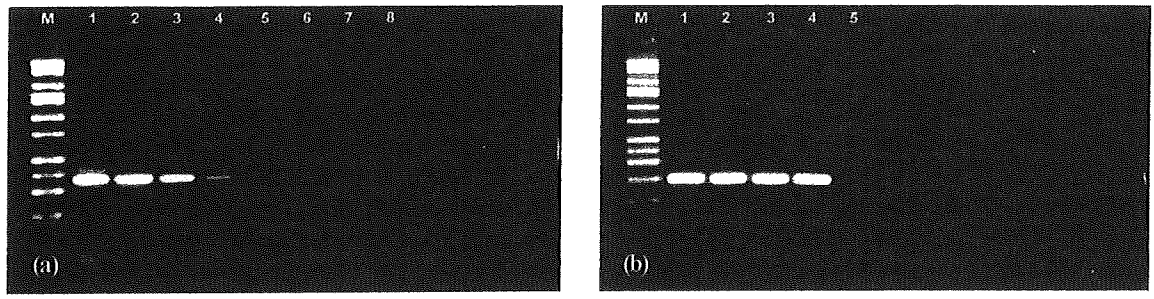

Fig. 1a: Sensitivity of the PCR assay for detection of *C. parvum* oocysts as determined by agarose gel electrophoresis. M: 100 bp ladder, Lane 1: positive control, Lane 2: 10^4 oocysts, Lane 3: 10^3 oocysts, Lane 4: 10^2 oocysts, Lane 5: 10 oocysts, Lane 6: 5 oocysts, Lane 7: 1 oocyst, Lane 8: negative control. b: Sensitivity of the nested- PCR assay. Lane 1: positive control, Lane 2: 10 oocysts, Lane 3: 5 oocysts, Lane 4: 1 oocyst, Lane 5: negative control.

Table 1: Comparison of results obtained by QIAamp-nested PCR and IMS-nested PCR for detection of *C. Parvum* oocysts in various water samples

Sample	Turbidity	Volume Analyzed	No. of seeded oocysts	Replicate	nested PCR detection	
					QIA amp	IMS
*Tap water	<1	10-60 L	0	6	-	**
		"	1	6	+	**
		"	5	6	+	+
		"	10	6	+	+
		"	100	3	+	**
River water	1.5	20	0	1	-	-
			5		+	+
River water	3.3	20	0	1	-	-
			5		-	-
River water	2.5	20	0	1	-	-
			5		-	-
River water	3.5	30	0	1	-	-
			5		-	+
			10		-	+
River water	1.7	20	0	1	-	-
			5		+	+
River water	2	20	0	1	-	-
			5		+	+
Stream water	1.9	15	0	1	-	**
			5		+	**
			10		+	**

*For IMS one replicate, **IMS not performed

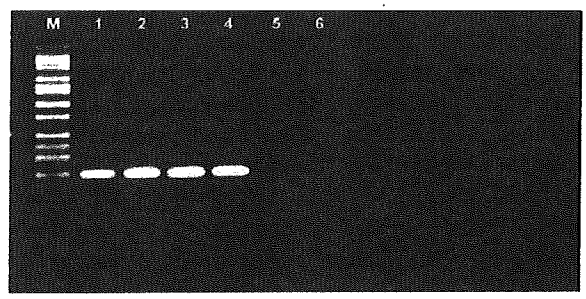

Fig. 2: Sensitivity of nested-PCR assay for detection of *C. parvum* oocysts spiked into packed pellet concentrates from 50 liters tap water samples after purification of DNA by QIAamp. M: 100 bp ladder, Lane 1: positive control, Lane 2: 10 oocysts, Lane 3: 5 oocysts, Lane 4: 1 oocyst, Lane 5: negative control without oocyst, Lane 6: negative control without DNA

Magnetic beads with attached oligonucleotides also have been used to isolate specific target nucleic acid (Kauncer and Stinear, 1998; Stinear, *et al.*, 1996). In this study we used a nested–PCR assay which further enhances the sensitivity of PCR for detection of *C. Parvum* oocysts. Nested PCR has been used with various degrees of success to increase the sensitivity of detection, particularly for genes with one or a small number of copies (Inglis and Kalischuk, 2003). The nested-PCR method also was able to detect low numbers of *C. parvum* oocysts spiked into tap water concentrates. QIAamp DNA mini kit overcame potential nested–PCR inhibition and proved to be an efficient DNA purification procedure for tap water samples. Although immunomagnetic separation (IMS) is now more commonly used and many researches have been used the method along with PCR for detection of *Cryptosporidium* oocysts in environmental samples (Hallier-Soulier and Guillot, 1996; Hallier-Soulier and Guillot, 2000; Rimhanen-finne, *et al.*, 2001; Sturbaum, *et al.*, 2002; Xiao, *et al.*, 2001), but the procedure selectively separate the *Cryptosporidium* oocysts. However it would be advantageous to perform parallel detection assay for multiple pathogen on a single sample. This can be accomplished by extraction of total DNA from a concentrated water sample without selective separation (Rochelle, *et al.*, 1997b). QIAamp has the advantage that will not selectively target the

DNA of any one organism and therefore potentially could be used for purification of DNA in detection of organisms in water samples by PCR.

As indicated by the results of this study, there is a discrepancy between the two methods. The discrepancy was due to the samples with turbidities higher than 2 NTU. Samples of this nature may be expected to contain higher level of debris and PCR inhibitors that might bind DNA immediately upon release from the target microbial cells. Moreover nested–PCR amplification of the two samples failed when IMS was used. The higher level of algae in these samples, take as a guide to the level of humic acid, may explain the failure. Lowery *et al.* (2000) indicated that the sensitivity of IMS– PCR for environmental water samples with turbidity between 2.5 and 5% ppv. is 100 fold lower than water samples with turbidity below 2.5% ppv.

In conclusion QIAamp DNA mini kit is a suitable procedure for purification of DNA in water samples with low turbidity (<2 NTU) especially tap water samples. The advantages of the method include reducing process time, expense and using the method for detection of any kind of microorganism by PCR - based methods.

ACKNOWLEDGEMENT

The authors thank NIID for providing the oocysts stock and Mrs.Yuko Takahashi for technical assistance.

REFERENCES

Awad-el-Kariem, F.M., Warhurst, D.C., McDonald, V., (1994). Detection and species identification of Cryptosporidium oocysts using a system based on PCR and endonuclease restriction. Parasitology. **109**, 19-22.

Carraway, M., Tzipori, S., Widmer, G., (1996). Identification of genetic heterogeneity in the *Cryptosporidium parvum* ribosomal repeat. Appl. Environ. Microbiol., **62**, 712-716.

De La Cruz, A.A., Sivaganesan, M., (1994). Detection of *Giardia* and *Cryptosporidium* spp. in source water samples by commercial enzyme-immunoassay kits. Proc. AWWA Water Qual. Technol. Conf.

Deng, M.Q., Cliver, D.O., Mariam, T.W., (1997). Immunomagnetic capture PCR to detect viable *Cryptosporidium parvum* oocysts from environmental samples. Appl. Environ. Microbiol. **63** (8), 3134-3138.

Dupont, H.L., Chappell, C.L., Sterling, C.R., Okhuysen, P.C. Rose, J.B., Jakubowski, W., (1995). The infectivity of *Cryptosporidium parvum* in healthy volunteers. New Engl. J. Med., **332**, 855-859.

Fayer, R., Ungar B.L.P., (1986). *Cryptosporidium* spp. and cryptosporidiosis. Microbiol. Rev., **50**, 458-483.

Fayer, R., Morgan, U., Upton, S.J., (2000). Epidemiology of *Cryptosporidium*: transmission, detection and identification. Int. J. Parasitol., **30**, 1305-1322.

Griffin, D.W., Rose J.B., (1995). The use of magnetic affinity cell sorting to enhance PCR detection of *Cryptosporidium* oocysts in environmental samples. Proc. AWWA Water Qual. Technol. Conf., 2231-2241.

Hallier-Soulier, S., Guillot, E., (1999). An immunomagnetic separation polymerase chain reaction assay for rapid and ultra-sensitive detection of *Cryptosporidium parvum* in drinking water. FEMS Microbiol. Lett., **176** (2), 285-289.

Hallier-Soulier, S., Guillot, E., (2000). Detection of cryptosporidia and *Cryptosporidium parvum* oocysts in environmental water samples by immunomagnetic separation-polymerase chain reaction. J. Appl. Microbiol., **89** (1), 5-10.

Inglis, G.D., Kalischuk, L.D., (2003). Use of PCR for direct detection of Campylobacter species in bovine feces. Appl. Environ. Microbiol., **69** (6), 3435-33447.

Johnson, D.W., Pieniazek, N.J., Griffin, D.W., Misener, L., Rose, J.B., (1995). Development of a PCR protocol for sensitive detection of *Cryptosporidium* oocysts in water samples. Appl. Environ. Microbiol., **61**, 3849-3855.

Kaucner, C., Stinear, T., (1998). Sensitive and rapid detection of viable *Giardia* cysts and *Cryptosporidium parvum* oocysts in large-volume water samples with wound fiberglass cartridge filters and reverse transcription-PCR. Appl. Environ. Microbiol., **64** (5), 1743-1749.

Korich, D.G., Mead, J.R., Madore, M.S., Sinclair, N.A., Sterling, C.R., (1990). Effects of ozone, chlorine dioxide, chlorine, and monochloramine on *Cryptosporidium parvum* oocyst viability. Appl. Environ. Microbiol., **56**, 1423-1428.

Kozwich, D., Johansen, K.A., Landau, K., Roehl, C.A., Woronoff, S., Roehl, P.A., (2000). Development of a novel, rapid integrated *Cryptosporidium parvum* detection assay. Appl. Environ. Microbiol., **66** (7), 2711-2717 .

LeChevallier, M.W., Di Giovanni, G.D., Clancy, J.L., Bukhari, Z., Bukhari, S., Rosen, J.S., Sobrinho, J., Frey, M.M., (2003). Comparison of Method 1623 and Cell Culture-PCR for Detection of *Cryptosporidium* spp. in Source Waters. Appl. Envir. Microbiol., **69**, 971-979

LeChevallier, M.W., Norton, W.D., (1995). *Giardia* and *Cryptosporidium* in raw and finished water. J. AWWA, **87**(9), 54-68.

LeChevallier, M.W., Norton, W.D., Lee, R.G., (1991). Occurrence of *Giardia* and *Cryptosporidium* spp. in surface water supplies. Appl. Environ. Microbiol., **57**, 2610-2616.

Lisle, J.T., Rose, J.B., (1995). *Cryptosporidium* contamination of water in the USA and UK: a mini-review. J. Water SRT - Aqua, **44** (3), 103-117.

Lowery, C.J., Moore, J.E., Millar, B.C., Burke, D.P., McCorry, K.A., Crothers, E., Dooley, J.S., (2000). Detection and speciation of *Cryptosporidium* spp. in environmental water samples by immunomagnetic separation, PCR and endonuclease restriction. J. Med. Microbiol., **49** (9), 779-785.

Mahbubani, M.H., Schaefer, F.W., Jones, D.D., Bej, A.K., (1998). Detection of *Giardia* in environmental waters by immuno-PCR amplification methods. Curr. Microbiol. **36**(2), 107-113.

Mayer, C.L., Palmer, C.J., (1996). Evaluation of PCR, nested PCR, and fluorescent antibodies for detection of *Giardia* and *Cryptosporidium* species in wastewater. Appl. Envir. Microbiol., **62** (6), 2081-2085

Rimhanen-Finne, R., Ronkainen, P., Hanninen, M.L., (2001). Simultaneous detection of *Cryptosporidium parvum* and *Giardia* in sewage sludge by IC-PCR. J. Appl. Microbiol., **91** (6), 1030-1035.

Rochelle, P.A., De Leon, R., Stewart, M.H., Wolfe, R.L. (1997a). Comparison of primers and optimization of PCR conditions for detection of *Cryptosporidium parvum* and *Giardia lamblia* in water. Appl. Environ. Microbiol., **63**(1), 106-111.

Rochelle, P.A., Ferguson, D.M., Handojo, T.J., De Leon, R., Stewart, M.H. and Wolfe, R.L., (1997b). An assay combining cell culture with reverse transcriptase PCR to detect and determine the infectivity of waterborne *Cryptosporidium parvum*. Appl. Environ. Microbiol., **63** (5), 2029-2037

Stinear, T., Matusan, A., Hines, K., Sandery, M., (1996). Detection of a single viable *Cryptosporidium parvum* oocyst in environmental water concentrates by reverse transcription-PCR. Appl. Environ. Microbiol., **62** (9), 3385-3390

Sturbaum, G.D., Klonicki, P.T., Marshall, M.M., Jost, B.H., Clay, B.L., Sterling, C.R., (2002). Immunomagnetic separation (IMS)-fluorescent antibody detection and IMS PCR detection of seeded *Cryptosporidium parvum* oocysts in natural waters and their limitations. Appl. Environ. Microbiol., **68** (6), 2991 2996.

Vesey, G., Hutton, P., Champion, A., Ashbolt, N., Williams, K.L., Warton, A., Veal, D., (1994). Application of flow cytometric methods for the routine detection of *Cryptosporidium* and *Giardia* in water. Cytometry. **16** (1), 1-6.

Xiao, L., Singh, A., Limor, J., Graczyk, T.K., Gradus, S., Lal, A., (2001). Molecular characterization of *Cryptosporidium* oocysts in samples of raw surface water and wastewaters. Appl. Envir. Microbiol., **67** (3), 1097-1101.

AUTHOR (S) BIOSKETCHES

Nikaeen, M., Ph.D., Assistant Professor in the Department of Environmental Health Engineering, School of Public Health, Isfahan University of Medical Sciences, Isfahan, Iran. Email: *nikaeen_m@yahoo.com*

Makimura, K., M.D., Ph.D., Professor in the Department of Molecular Biology and Gene Diagnosis, Teikyo University, Tokyo, Japan. Email: *makimura@main.teikyo-u.ac.jp*

This article should be referenced as follows:

Nikaeen, M., Makimura, K., (2007). Evaluation of QIAamp DNA mini kit for removing of inhibitors in detection of Cryptosporidium parvum Oocysts in water samples by a nested-PCR assay. Int. J. Environ. Sci. Tech., 4 (2), 241-246.

Original Article

Antifungal drug susceptibility of *Cryptococcus neoformans* from clinical sources in Nairobi, Kenya

Christine C. Bii,[1,2] Koichi Makimura,[3] Shigeru Abe,[3] Haruhiko Taguchi,[2] Olga M. Mugasia,[1] Gutura Revathi,[4] Njeri C. Wamae[1] and Shigeru Kamiya[2]

[1]*Mycology Laboratory, Center for Microbiology Research, Kenya Medical Research Institute, Nairobi, Kenya,* [2]*Division of Medical Microbiology, Department of Infectious Diseases, Kyorin University School of Medicine, Tokyo, Japan,* [3]*Genome Research Centre and Institute of Medical Mycology, Teikyo University, Tokyo, Japan and* [4]*Kenyatta National Hospital, Nairobi, Kenya*

Summary

The serotypes and mating types of 80 clinical isolates of *Cryptococcus neoformans* from Kenya were studied and subjected to broth microdilution susceptibility testing to amphotericin B (AMP), flucytosin, fluconazole (FLC), itraconazole (ITC) and miconazole (MCZ). The isolates included *C. neoformans* var. *grubii* – 75 of 80 (serotype A; 93.7%), *C. neoformans* var. *neoformans* – three of 80 (3.8%) and *C. neoformans* var. *gattii* – two (serotype B; 2.5%). Mating experiment confirmed all the isolates to be α-mating type. Seventy-eight (97.5%) of the isolates had minimum inhibitory concentration (MIC) of ≤0.5 μg ml^{-1} to AMP and at 1 μg ml^{-1}, 100% of the isolates were inhibited. Flucytosin resistance was observed in 21% with MIC in which 90% of the isolates were inhibited (MIC_{90}) of 64 μg ml^{-1}. Only 23.8% of the strains were susceptible to FLC with 65% susceptible dose-dependent (SDD) and 11.2% resistant. Itraconazole susceptibility was 61.3% while the rest were either SDD or resistant. The MIC_{90} for ITC and MCZ were 0.5 and 2 μg ml^{-1} respectively.

The study reports the serotypes, mating types and highlights the existence of azoles resistance in *C. neoformans* in Nairobi which calls for antifungal drug resistance surveillance as prophylactic use of FLC increases because of human immunodeficiency virus/acquired immunodeficiency syndrome (HIV/AIDS) epidemic in sub-Saharan Africa.

Key words: serotypes, resistance, *Cryptococcus neoformans*, Kenya.

Introduction

Human immunodeficiency virus (HIV) epidemic has led to a growing population of immunocompromised patients at risk of contracting opportunistic fungal infections particularly cryptococcosis.[1] Globally, the risk for cryptococcal meningitis HIV/acquired immunodeficiency syndrome (AIDS) is estimated at 6–8% in adults and 1% in children.[2,3] In sub-Saharan Africa which has the highest burden of HIV/AIDS worldwide, the incidence of meningoencephalitis has increased significantly with mortality higher than meningococcal meningitis caused by *Neisseria meningitidis*.[4,5]

Cryptococcus neoformans consist of serotypes, A, B, C, D and AD classified into three varieties: *C. neoformans* var. *neoformans* (serotype D), *C. neoformans* var. *grubii* (serotype A) both of the teleomorph *Filobasidiella neoformans* var. *neoformans* and *C. neoformans* var. *gattii* (serotypes B and C) of the teleomorph *F. neoformans* var. *bacillisporus*.[6,7] The prevalence and geographical distribution of the two varieties vary. Generally, *C. neoformans* var. *neoformans* is the most prevalent with worldwide distribution while *C. neoformans* var. *gattii* is limited to tropics and subtropical regions coinciding with the distribution of the host trees *Eucalyptus camaldulensis* and *E. tereticornis*.[8] Distinct genotype clusters among isolates of African, America and Europe

Correspondence: Christine C. Bii, Mycology Laboratory, Kenya Medical Research Institute, PO Box 2632, 00202 Nairobi, Kenya.
Tel: 254 2724264. Fax: 254 2720030.
E-mail: kiptobi@yahoo.com

Accepted for publication 26 June 2006

doi:10.1111/j.0933-7407.2006.01293.x

origin may exist[9–11] but whether this is clinically relevant in terms of drug susceptibility and virulence-related factors remain unclear.

Despite the World Health Organization (WHO) initiatives on antimicrobial resistance surveillance, antifungal drug resistance surveillance in sub-Saharan Africa remains somewhat ignored. While improvement in susceptibility to antifungal drugs was recently reported in Europe and the USA,[12] the need for life-long fluconazole (FLC) maintenance therapy due to high relapse rates of cryptococcosis in HIV/AIDS raises concerns over antifungal resistance in developing countries.[13,14] As FLC becomes widely used due to expanding population of HIV/AIDS confounded by irrational use of antibiotics, and generic antibiotics in developing countries, emergence azole resistance cannot be inevitably ignored as a mycological challenge.[15] The study was undertaken to characterise *C. neoformans* serotypes and antifungal drug susceptibilities essential for a mounting appropriate clinical management for cryptococcal infection in HIV/AIDS in Kenya.

Materials and methods

Cryptococcus strains

Eighty *C. neoformans* isolates from cerebral spinal fluids (CSF) specimens of adult patients hospitalised with cryptococcal meningitis from two referral hospitals in Nairobi, Kenya were used in the study. The specimens were collected from individual patients before therapy was initiated. Between January 2003 and January 2004 72 strains from HIV-positive patients and eight from patients with unknown HIV status were isolated at Mycology Laboratory, Kenya Medical Research Institute. Primary isolation was underwent on Sabourauds dextrose agar incubated at 30 °C for 72 h and preliminary identification was performed by demonstration of capsule on Indian ink.

Biochemical and immunological characterisation

All the isolates were subcultured on CHROMagar Candida (CHROMagar, Paris, France) to rule out contamination and to ensure purity of the isolates by its ability to discriminate *Candida* spp. Confirmation of *C. neoformans* was carried out by Vitek Yeast Biochemical Cards (bioMerieux-Vitek, Hazelwood, MO, USA). Serotypes were determined by slide agglutination test using Crypto Check agglutination kit (Iatron Labs Inc., Tokyo, Japan).

Mating experiment

The mating types (MAT) were determined as described previously.[7] Authentic strains: *C. neoformans* TLD-350 serotype A, MATα, *C. neofomans* TLD-261 serotype D, MATα, *C. neoformans* TLD-262 serotype D, MAT*a*, *C. neoformans* TLD-263 serotype B, MATα and *C. neoformans* TLD-264 serotype C, MATα were used. Briefly, individual isolates were co-cultured with the tester strain in an agar medium containing KH_2PO_4, $MgSO_4$, $CaCl_2$, NaCl, biotin, sucrose and yeast extract and incubated at 30 °C for 20 days. Mating was considered successful when mycelia with characteristic clamp connection were observed.

Antifungal drug susceptibility

Cryptococcus isolates were subjected to broth microdilution susceptibility test using commercial Frozen Plate Kit (Eiken Chemical Co., Ltd, Tokyo, Japan).[16] The Kit contains the following drug dilution ranges: amphotericin B (AMP) 0.03–16 μg ml^{-1}, flucytosin (5FC) 0.125–64 μg ml^{-1}, FLC 0.125–64 μg ml^{-1}, itraconazole (ITC) 0.015–8 μg ml^{-1}, miconazole (MCZ) 0.06–32 μg ml^{-1} and micafungin (MCFG) 0.03–16 μg ml^{-1}. The Kit has been evaluated in a multicentre study with over 90% agreement with CLSI.[17,18] The procedures and minimum inhibitory concentrations (MIC) were carried out and interpreted according to the manufacturer's instructions. The MIC for azoles and 5FC were scored as the lowest drug concentration that resulted in 80% growth inhibition (IC_{80}) while 100% reduction of turbidity was considered MIC for AMP. Quality control was performed using *Candida krusei* ATCC 6258 and *C. parapsilosis* ATCC 22019 and results excepted only if the MIC were within the recommended range.

The study protocol was approved by the Kenya Medical Research Institute ethical and scientific steering committee (SSC) before implementation and was assigned SSC number 766. The procedures conformed to all the scientific and ethical standards during its implementation.

Results

Identification and typing

Seventy-five of 80 (93.7%) isolates were identified as *C. neoformans* var. *grubii* (serotype A). Only three isolates were identified as *C. neoformans* var. *neoformans* (two serotype AD and one serotype D) while two

isolates were identified as *C. neoformans* var. *gattii* (serotype B); however, all the isolates were identified as MATα.

Drug susceptibility

All the isolates were susceptible to AMP with MIC_{90} of 0.5 μg ml^{-1} and only two isolates with MIC of 1 μg ml^{-1} (Table 1). All except one isolate had MIC beyond susceptible level (MIC ≤4 μg ml^{-1}) to 5FC while 77.6% of the isolates had MIC ranging from 8 to 32 μg ml^{-1}. Resistance (MIC ≥ 64 μg ml^{-1}) to 5FC was 21.2%. The MIC_{90} for 5FC and FLC was 64 μg ml^{-1} each. Nine of 80 (11.2%) isolates were resistant (MIC ≥64 μg ml^{-1}) to FLC while 52 of 80 (65.0%) were categorised as susceptible dose-dependent (SDD; MIC 16–32 μg ml^{-1}). Among the azoles tested, ITC had the lowest MIC_{90} similar (0.5 μg ml^{-1}) to that of AMP; however, there were three isolates with MIC ≥8 μg ml^{-1} to ITC. Only seven of 80 (8.8%) of the isolates were fully susceptible (MIC ≤0.125 μg ml^{-1}) to MCZ, 62 of 80 (77.5%) were SDD (MIC 0.25–1 μg ml^{-1}) and 11 of 80 (13.7%) were resistant (MIC >1 μg ml^{-1}). The MIC_{90} for MCZ was 2 μg ml^{-1}. The only isolate identified as serotype D exhibited MIC beyond susceptible range to all except AMP with MICs (μg ml^{-1}) as follows: AMP 0.5, 5FC >64, FLC >64, ITC >8 and MCZ 8. All the isolates tested were resistant (MIC ≥16 μg ml^{-1}) to MCFG (data not shown).

Discussion

Cryptococcus neoformans var. *grubii* (serotype A) MATα was the predominant isolate with evidence of azole resistance. This is in consistent with other reports of the worldwide distribution of this serotype and its predilection for HIV/AIDS.[1] Two isolates of serotype AD and one serotype D were identified indicating the infrequent cause of these serotypes in cryptococcoses in accord with reports that African patients are rarely infected with *C. neoformans* var. *neoformans* serotype D.[19] Two strains of *C. neoformans* var. *gattii* (serotype B) were identified, although this serotype rarely infects HIV/AIDS patients, the two strains were recovered from patients whose HIV status was unavailable. *Cryptococcus neoformans* var. *gattii* is predominant in tropical and subtropical areas coinciding with the distribution of the host tree, the *Eucalyptus* species.[8,20] These trees are now widely grown in Kenya for its timber products and that could have an influence on the presence of this serotype in Kenya. Nonetheless, the study confirms the existence of *C. neoformans* var. *gattii* (serotype B) in Kenya and it would be important to ascertain its clinical significance.

Despite evidence of sexual recombination among *C. neoformans* in sub-Saharan Africa,[21] all the strains were identified as MATα-type, which further supports the hypothesised predominance of MATα over MAT*a* in both clinical and natural environment.[22] The prevalence and virulence of *C. neoformans* has been linked to mating types. Pathogenic strains are largely asexual[23]

Table 1 Antifungal drug susceptibility of *Cryptococcus neoformans* isolates from Kenya

Antifungal drug concentration (μg ml^{-1})	Number of susceptible isolates (%)				
	Amphotericin B	Flucytosin	Fluconazole	Itraconazole	Miconazole
0.06	0 (0)	0 (0)	0 (0)	29 (36.3)	5 (6.2)
0.125	10 (12.5)	0 (0)	0 (0)	20 (25.0)	2 (2.5)
0.25	27 (33.8)	0 (0)	0 (0)	19 (23.8)	15 (18.8)
0.5	41 (51.2)	1 (1.2)	0 (0)	7 (8.8)	35 (43.8)
1	2 (2.5)	0 (0)	1 (1.2)	2 (2.5)	12 (15.0)
2	0 (0)	0 (0)	3 (3.8)	0 (0)	5 (6.2)
4	0 (0)	0 (0)	3 (3.8)	0 (0)	4 (5.0)
8	0 (0)	15 (18.8)	12 (15.0)	3 (3.8)	2 (2.5)
16	0 (0)	23 (28.8)	46 (57.5)	–	0 (0)
32	–	24 (30)	6 (7.5)	–	0 (0)
64	–	17 (21.2)	9 (11.2)	–	–
MIC_{50} (%)	0.5	64	16	0.125	0.5
MIC_{90} (%)	0.5	64	64	0.5	2
MIC of *Candida parapsilosis* ATCC 22019	0.25	0.5	0.5	0.25	2
MIC of *Candida krusei* ATCC 6258	1	16	32	0.25	2

MIC_{90}: concentration at which 90% of the isolates were inhibited.

Horizontal line show beyond dilution range tested.

